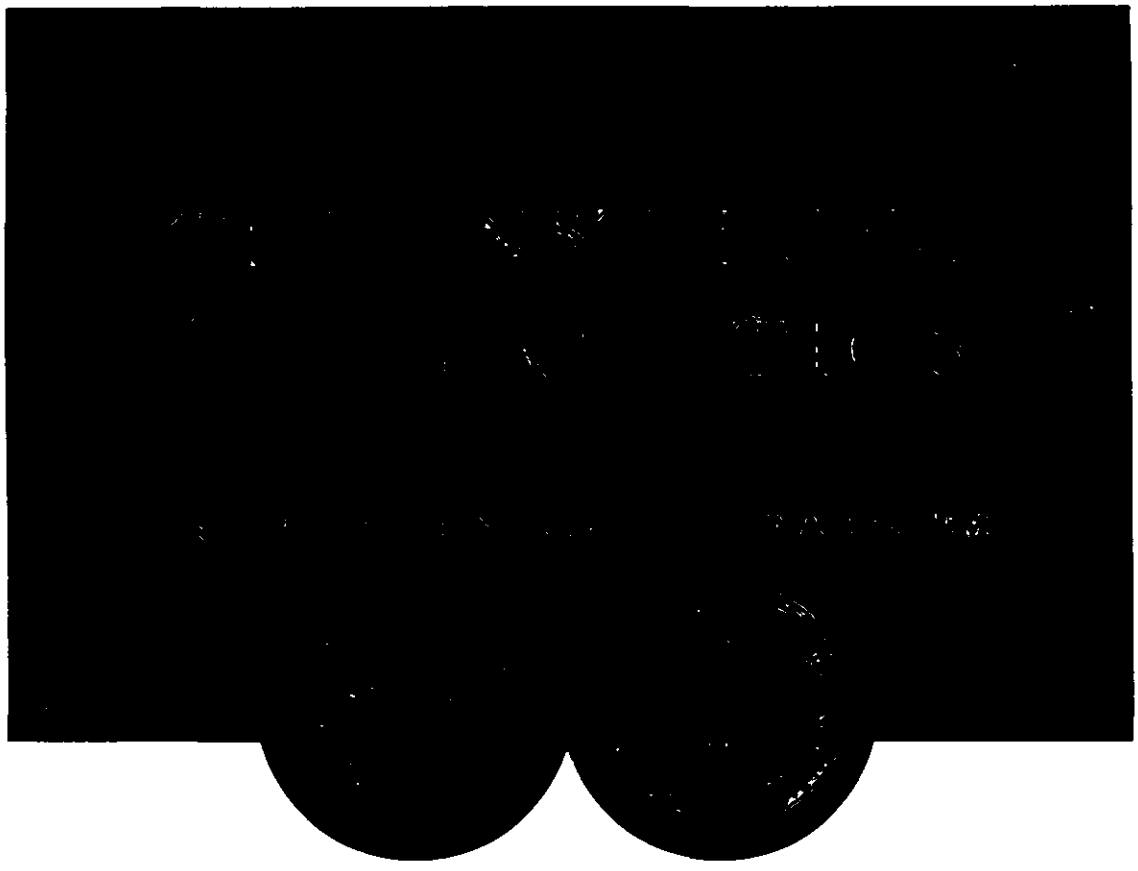

Response characteristics of a simple neuronal oscillator to a periodic input in noisy environment - an analysis of stochastic phase lockings and stochastic bifurcations

Shinji Doi, Junko Inoue, Shunsuke Sato and Charles E. Smith

Institute of Statistics Mimeo Series #2299

NORTH CAROLINA STATE UNIVERSITY
Raleigh, North Carolina

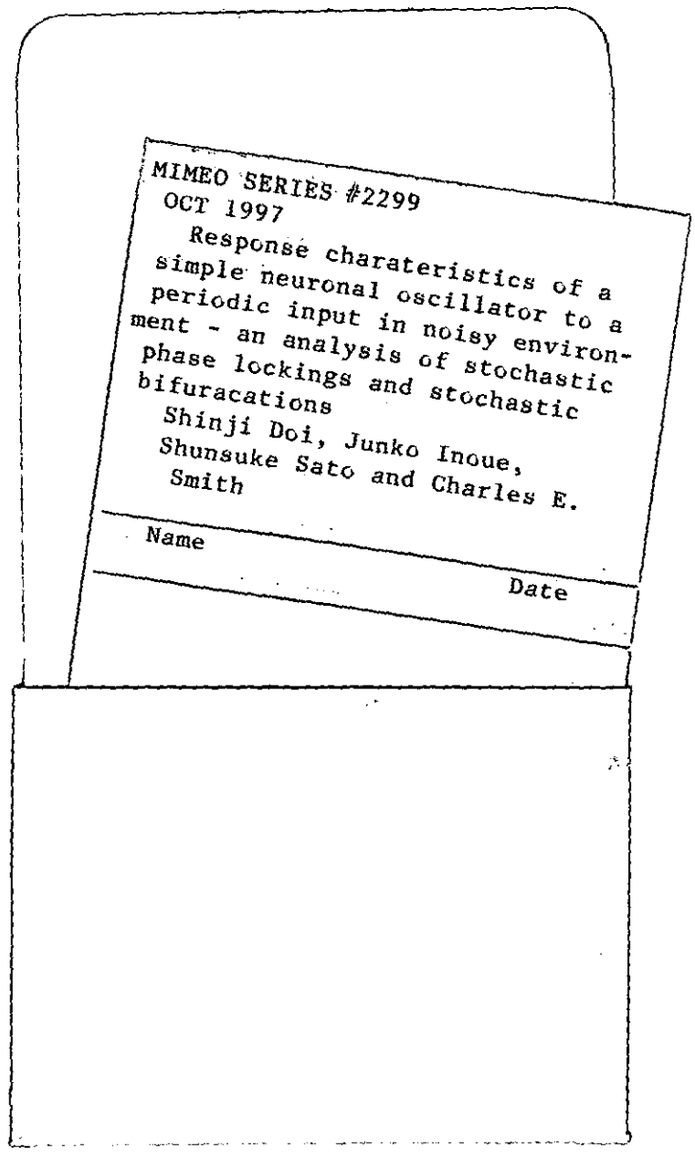
MIMEO SERIES #2299
OCT 1997
Response charateristics of a simple neuronal oscillator to a periodic input in noisy environment - an analysis of stochastic phase lockings and stochastic bifuracations
Shinji Doi, Junko Inoue, Shunsuke Sato and Charles E. Smith
Name
Date

Response characteristics of a simple neuronal oscillator to a periodic input in noisy environment — an analysis of stochastic phase lockings and stochastic bifurcations —

Shinji Doi†, Junko Inoue‡, Shunsuke Sato* and Charles E. Smith*

†Faculty of Engineering, Osaka University, Suita, Osaka 565, Japan,

e-mail: doi@pwr.eng.osaka-u.ac.jp

‡Institute for Information Processing, Koka Women's College

⋆ Faculty of Engineering Science, Osaka University

∗ Department of Statistics, North Carolina State University

ABSTRACT

A van der Pol relaxation (slow-fast) oscillator is considered as a simple model of a neuronal oscillator. When the input to the oscillator is a sinusoidal signal, the oscillator shows various patterns of phase lockings depending on the period and amplitude of the input. Noise effects on the phase lockings and bifurcations in the forced oscillator are investigated. The deterministic (noise-free) one-dimensional mapping is extended to the iteration of the operator defined by a stochastic kernel function. Stochastic phase lockings and bifurcations are analyzed in terms of the density evolution by the operator and its spectral characteristics.

1 Introduction

Various rhythmic phenomena are found and considered to play an important role in the temporal organization of biological systems (Glass and Mackey 1988). A physical system such a cardiac pacemaker(s) which presents a spontaneous periodicity is called a oscillator. Such a oscillator is mathematically considered to be a nonlinear oscillator since its rhythmicity is stable against external small perturbations. A so-called relaxation oscillator (Grasman 1987) has two different time scales; slow and fast dynamics. Dynamics with multiple time scales are typical in biological systems, especially in neuronal systems. Such a relaxation oscillator has a long history as a model of a biological oscillator (van der Pol 1929, Grasman and Jansen 1979). The van der Pol oscillator provides a prototypical example of a nonlinear oscillator and represents the relaxation oscillation in the limit of high nonlinearity (Guckenheimer and Holmes 1983).

An oscillator changes its periodicity when influenced by other oscillators. An oscillator which governs a circadian rhythm such as a sleep-wake cycle might be influenced by a environmental periodicity such as the 24 hours-cycle of a day and a cardiac pacemaker cell(s) is affected by a signal from a central nervous system (Noble 1975). Electrical signals from the pacemaker cells at the sino-atrial node of a heart are transmitted to the Purkinje fiber, which has a spontaneous periodicity also, and can be considered as a forced oscillator.

Numerous studies on such a forced nonlinear oscillator, including the van der Pol equation, have been performed (many articles are included in (Kapitaniak 1991)). If the amplitude of the external force (or the driver) is sufficiently large, the forced (or drived) oscillator is entrained, or phase-locked, or synchronized to the external force. When a driving period T is in the neighborhood of the characteristic period of the free oscillator, one may expect

an entrained oscillation at the driving period; this is called a $1:1$ phase-locking. On the other hand, even though the period of the system is relevantly different from the driving period, phase lockings occur: the period of the system is entrained to a period which is an integral multiple or submultiple of the driving period. As the period and/or amplitude of the driver are varied, the driven oscillator may show an $m:n$ phase locking in which the driven oscillator runs n cycles for each m cycles of the driver.

An oscillator is mathematically described by a set of (nonlinear) differential equations and considered to be a (nonlinear) dynamical system (Guckenheimer and Holmes 1983). The influence of noise on nonlinear dynamical systems has been an object of intense investigations (Moss and McClintock 1987) since real systems, especially biological systems, always have noise. The phenomenon of transitions induced by external noise has led to a revival of the interest for the role of fluctuations in physical systems (Horsthemke and Lefever 1984). For instance, in a multi-stable system which possesses several competing states of local stability, noise can be responsible for transitions between these states. Recently "noisy" systems have also received considerable attention within the context of stochastic resonance (see the reference [1]). Grasman and Roerdink (1989) analyzed the van der Pol relaxation oscillator with additive noise and reduced the problem of examining the period of the noisy oscillator to the analysis of the time necessary for a one-dimensional stochastic process to reach a boundary for the first time (a first-passage time).

We consider the (piecewise-linearized) van der Pol relaxation oscillator and its slight modification (a simple case of the Bonhoeffer-van der Pol or FitzHugh-Nagumo neuronal model (FitzHugh 1961)) as a simple model of a neuronal oscillator. The Bonhoeffer-van der Pol model is well known to be a simplified model of the Hodgkin-Huxley equation (Hodgkin

and Huxley 1952). The relaxation oscillator forced by a sinusoidal input displays various phase-locking patterns if some control parameters such as the amplitude and/or period of the periodic input are changed. A phase-locking pattern is considered to be bifurcated from an another phase-locking pattern as a control parameter (bifurcation parameter) changes. A bifurcation is a typical phenomenon in nonlinear dynamical systems and a bifurcation analysis is a useful method to analyze nonlinear dynamical systems (Guckenheimer and Holmes 1983).

This article analyzes noise effects on the phase lockings and the bifurcations. Section 2 presents the van der Pol model. The sinusoidally-forced van der Pol oscillator in the absence of noise is analyzed using a one-dimensional (Poincaré) mapping of a 'phase' variable and examples of (deterministic) phase lockings and bifurcations are presented in Sect. 3. Section 4 analyzes the forced oscillator with noise. The Grasman's first-passage-time approach mentioned above is extended to the presence case of a sinusoidal input (Tateno *et al.* 1995). In the presence of noise, the one-dimensional map is extended to a stochastic kernel function, and the iteration of the map is extended to an iteration of an operator defined by the stochastic kernel function. In Sect. 5, noise effects on the phase lockings and bifurcations are analyzed in terms of the sequence of probability density functions produced by the operator. Section 6 presents a new framework which analyzes the stochastic bifurcations from the viewpoint of the spectral properties (eigenvalues and eigenfunctions) of the operator.

2 van-der Pol Relaxation Oscillator

We consider the (piecewisely linearized) van der Pol oscillator and its slight modification (a simple version of the Bonhoeffer-van der Pol or FitzHugh-Nagumo neuronal model (FitzHugh 1961)) in the presence of both a sinusoidal forcing and noise:

$$\epsilon \frac{dX(t)}{dt} = f(X(t), Y(t)), \tag{1a}$$

$$\frac{dY(t)}{dt} = -X(t) + a + v(t) + \sigma \frac{dW(t)}{dt} \tag{1b}$$

$$f(x, y) = y - x + 5/6\{|x + 1| - |x - 1|\}$$

$$v(t) = A \sin\{2\pi(t/T + \theta_0)\}$$

where A, T, θ_0 are the amplitude, the period, the initial phase of the sinusoidal input, respectively. $W(t)$ is the standard Wiener process (Gardiner 1983) and $\sigma dW(t)/dt$ denotes a Gaussian white noise with a noise intensity σ. The variable X corresponds to the membrane potential of a neuron and Y some other property of a neuron such as refractoriness. $X < 0$ means that a membrane potential is sub-threshold and $X > 0$ supra-threshold (depolarized). The parameter a controls the asymmetry of the model and the $a = 0$ case corresponds to the original van der Pol oscillator. We also call this slightly modified van der Pol oscillator as simply the van der Pol oscillator and the van der Pol oscillator without any mention of the a value usually means the original van der Pol oscillator ($a = 0$).

We consider a limit of $\epsilon = 0$. In this case, the van-der Pol oscillator shows a so-called relaxation oscillation. Figure 1 shows the x-y phase plane of eq. (1). The solution (X, Y) of eq. (1) is called the state point of the oscillator. In the case of $\epsilon = 0$, the state point moves along the closed curve ABCD with the speed of the state point modulated by both the sinusoidal input and noise. At the points B and D, the state point (instantaneously)

jumps to the points C and A, respectively, since we consider the singular limit of $\epsilon = 0$.

Figure 2 shows the time course of $X(t)$ without noise and without a sinusoidal input. The solid curve is the $a = 0$ case and the broken curve the $a = -0.5$ case. Both waveforms have a 'plateau' such as that of cardiac cells (Noble 1975). As the value of a decreases, the asymmetry of the waveform is increased and the depolarized ($X(t) > 0$) fraction of time in one cycle (period) decreases. This fraction of time is called an activity and the importance of asymmetry is already noted in the context of coupled oscillators (Kepler *et al.* 1990, Meunier 1992).

3 Deterministic Phase Lockings Without Noise

3.1 Poincaré mapping

This section consider the noise-free case ($\sigma = 0$). In order to study the relation between the sinusoidal forcing and the forced oscillator, let us observe the sinusoidal input whenever the state point (X,Y) visits the point A of the x-y phase plane (see Fig.1). Figure 3 is an example of waveforms of both the sinusoidal input and the oscillator. The point A of the x-y phase plane corresponds to the peaks of the oscillator waveform $X(t)$. The phase of the sinusoidal input (at the point A) is a number between 0 and 1 normalized by the period T (c.f. Fig.3). Suppose that the state point starts at the point A of the x-y phase plane with an initial phase θ_0 and that the state point returns to the point A again after a time t_1. Then the second phase θ_1 is obtained by

$$\theta_1 = p(\theta_0) \stackrel{\text{def}}{=} \theta_0 + t_1/T \qquad (\text{mod } 1). \tag{2}$$

The relation $p(\theta_0)$ between θ_0 and θ_1 is called a Poincaré map.

Using the Poincaré map, phases θ_2, θ_3, ... are recursively defined by the one-dimensional mapping:

$$\theta_{n+1} = p(\theta_n), \quad n = 0, 1, 2, ... \tag{3}$$

The sequence $\{\theta_n\}$ generated by this equation is also called the orbit of eq. (3).

Thus, in order to analyze the phase lockings of the noise-free case, we investigate the asymptotic properties of the sequence $\{\theta_n\}$ of phases. In Fig.3, the sequence $\{\theta_n\}$ asymptotically approaches a certain values θ^*; in this case a 1:1 locking occurs. Figure 4 shows an example of the Poincaré map $p(\theta)$ and its orbit $\{\theta_n\}$ which corresponds to Fig.3. The graph of $p(\theta)$ intersects with a diagonal line in two points (indistinguishable in this figure) and the lower intersection point θ^* is a stable fixed point of eq. (3). Thus an orbit θ_0, θ_1, ..., with any initial phase θ_0 asymptotically converges to this fixed point θ^*, which shows a 1:1 phase locking occurs.

Generally, in the case of m:n locking, an orbit or sequence $\{\theta_n\}$ asymptotically approaches to an n-periodic sequence:

$$\theta^{(1)}, \theta^{(2)}, ..., \theta^{(n)}, \theta^{(1)}, ...$$

3.2 Deterministic bifurcation diagrams

Patterns of phase-lockings depend on both the amplitude and the period of the sinusoidal input. Figure 5 shows how the asymptotic value(s) of the sequence $\{\theta_n\}$ is changed depending on the input period T. Part (a) is a bifurcation diagram of $a = 0.0$ (original van der Pol) oscillator. For example, in the $T = 2$ case, one dot is plotted in the vertical direction; a 1:1 locking occurs. In the $T = 7$ case, three dots are plotted and a 1:3 locking

occurs; one cycle of the sinusoidal input synchronize with three cycles of the oscillator. In the $T = 4$ case, many points are plotted; no locking occurs (in this case, the sequence $\{\theta_n\}$ approaches a so-called quasi-periodic sequence rather than a periodic sequence). In a quasi-periodic case, the oscillator is not phase-locked to the input and the phase of the input takes infinitely many values between 0 and 1 although the oscillator seems to be locked for a short time range.

In part (b), the value of a is set to -0.5. As shown in Sect. 2, the asymmetry of the waveform increases if the absolute value of a increases. The larger the absolute value of the parameter a becomes, the narrower the T range of quasi-periodic orbits becomes, although the total bifurcation structure (1:1, 1:3 lockings of (a)) does not change much. From this observation, we can see that the asymmetry (neuronality?) of a oscillator increases the tendency to phase lockings. We note that the intrinsic period T_a^{Int} of the van der Pol free (A=0, σ=0) oscillator is given by

$$T_a^{\mathrm{Int}} = \ln \frac{(7/3)^2 - a^2}{1 - a^2}$$

and does not change much for this range of parameter a:

$$T_{0.0}^{\mathrm{Int}} = 1.69, \quad T_{\pm 0.3}^{\mathrm{Int}} = 1.77, \quad T_{\pm 0.5}^{\mathrm{Int}} = 1.94$$

Thus the difference between (a) and (b) is caused by not the difference of intrinsic period but by the asymmetry.

4 Stochastic Phase Lockings With Noise

4.1 Stochastic kernel and Markov operator

In the noisy case, both variables θ_0, θ_1 defined in eq. (2) fluctuate by noise and are thus random variables Θ_0, Θ_1. We extend the deterministic map $p(\theta)$ to the case with noise as follows. Define a kernel function $g(\theta_0, \theta_1)$ using conditional probability density functions:

$$g(\theta_0, \theta_1)d\theta_1 = \Pr\{\theta_1 \leq \Theta_1 \leq \theta_1 + d\theta_1 \mid \Theta_0 = \theta_0\} \tag{4}$$

The function $g(\theta_0, \theta_1)$ can be calculated numerically without simulations of the stochastic differential equations (1) (Tateno *et al.*).

Figure 6 is an example of the kernel function g which corresponds to the deterministic Poincaré map of Fig.4. The function g takes relatively high values along the curves of the Poincaré map p. Thus g can be considered as the stochastic extension of the deterministic Poincaré map. The heights and widths of the peaks of g depends on the values of (θ_0, θ_1) and thus we can see that the effects of blurring of the deterministic map by noise are not uniform.

Using the kernel function g, we extend the system (3) to the noisy case as follows. Let S denote a unit interval [0,1] and $\mathcal{D}$ the set of absolutely integrable functions with a unit L^1 norm on S. An operator $\mathcal{P}$ on $\mathcal{D}$ is defined by:

$$\mathcal{P}h\,(\theta) = \int_S g(\theta_0, \theta)h(\theta_0)d\theta_0, \quad h \in \mathcal{D} \tag{5}$$

This operator is called a Markov operator since it transforms a probability density function to an another probability density function (Lasota and Mackey 1994). Let $h_0(\theta) \in \mathcal{D}$ denote

the probability density function of the initial phase Θ_0 when a state point starts at the point A of the x-y phase plane. Then the density function of Θ_1 when the state point returns to the point A again is obtained by $h_1(\theta) = \mathcal{P}h_0(\theta)$. Thus, the deterministic mapping (3) is extended to the system

$$h_{n+1}(\theta) = \mathcal{P}h_n(\theta), \quad n = 0, 1, 2, ... \tag{6}$$

Thus we investigate the asymptotic behavior of the sequence $\{h_n(\theta)\}$ of probability density functions rather than the sequence $\{\theta_n\}$ of phases.

Let us list several preliminary definitions (Lasota and Mackey 1994). A function $h^*(\theta)$ is called the *invariant density* function of an operator $\mathcal{P}$ if the relation $\mathcal{P}h^* = h^*$ holds. The invariant density is *asymptotically stable* if for any initial density function $h_0 \in \mathcal{D}$

$$\lim_{n\to\infty} ||\mathcal{P}^n h_0 - h^*|| = 0.$$

As is easily seen from its definition, the function g has the property

$$g(\theta_0, \theta_1) \geq 0, \qquad \int_S g(\theta_0, \theta_1) d\theta_1 = 1$$

and is called a stochastic kernel. The inequality

$$\int_S \inf_{\theta_0} g(\theta_0, \theta_1) d\theta_1 > 0 \tag{7}$$

is assumed to hold (Tateno *et al.* 1995). The operator with this property has a unique asymptotically stable invariant density (Lasota and Mackey 1994). Thus the sequence $\{h_n(\theta)\}$ produced by the operator $\mathcal{P}$ asymptotically approaches a unique invariant density as $n \to \infty$. The invariant density is considered as the stationary probability density function of the phase Θ_n.

Figure 7 is an example of the density sequence $\{h_n(\theta)\}$. The uniform initial density function $h_0(\theta)$ changes its shape and approaches an invariant density function h^* ($\approx h_{30}$)

with one sharp peak, which shows a 1:1 phase locking does occur in a stochastic sense. The peak of the density functions $\{h_n(\theta)\}$ is highest near $n = 7$ and is relatively lower in the invariant density h^*, which means that fluctuations of phases are bigger in the stationary state than in the transient state. This phenomenon is due to the fact that the peaks of the kernel function $g(\theta)$ near $\theta = \theta^*$ are relatively lower than the other (c.f. Fig.6 and Fig.4).

Figure 8 (a) is also an example of the density sequence in the case of stochastic 5:3 phase locking. The initial density function $h_0(\theta)$ has a high mode near $\theta = 0.42$ which is one of the three phases to which oscillator is locked in the noise-free case. The functions h_1 and h_2 have a high mode near the other two phases of the three phases. This sequence seems to initially vary with period 3, but finally converges to an invariant density function (part (b)) with three sharp peaks, which shows a 5:3 locking occurs in a stochastic sense.

5 Stochastic Bifurcation Diagram

Patterns of deterministic phase lockings depend on both the amplitude A and the period T of the input. Figure 9 shows a deterministic bifurcation diagram of the Poincaré map p for the noise-free (σ=0) case with a bifurcation parameter A rather than T (c.f. Fig.5). In this case, the period of the sinusoidal input is about a half of the intrinsic period of the van der Pol oscillator. So, for a wide range of the amplitude A, 2:1 phase lockings are shown (two cycles of the input synchronize with one cycle of the oscillator). In particular, two different patterns of 2:1 phase lockings coexist; the pattern depends on both the initial phase of the input and the initial state of the oscillator.

Various phase-locking patterns are bifurcated as the value of A varies. If A is large enough ($A > 2.4$), one cycle of the input can synchronize with the one cycle of the oscillator

although the intrinsic periods differ by twice.

Figure 10 is a stochastic or a density bifurcation diagram which corresponds to the deterministic one (Fig.9). Invariant density functions are plotted with various value of A for two different noise intensities $\sigma = 0.05$ and $\sigma = 0.2$. In the part (a), corresponding to the deterministic bifurcation diagram, the modes and the shape of the invariant density are changed as the bifurcation parameter A varies. Particularly, in the range of $1.8 < A < 2.4$, the invariant densities have several peaks and complicated shapes although the shapes are not so complicated as the deterministic one.

In the case of large noise (part (b)), the stochastic bifurcation diagram is very simple; the invariant densities have at most two peaks. The shapes of invariant densities do not depend on the amplitude A; only the heights of the two peaks depend on A. Thus noise washes out the dependency of the densities on the amplitude of the input.

In the deterministic dynamical systems, the word 'bifurcation' means qualitative change (number, stability) of solutions of a system. As stated above, the equation

$$\mathcal{P}h^* = h^*$$

which the invariant density satisfies, always has a unique asymptotically stable solution and thus no bifurcation of this equation occurs in such a sense. So what is a stochastic bifurcation? This is a newly developing field (Arnold 1995). One (classical) definition of stochastic bifurcation is based on the 'shape' of invariant density functions.

For example, near $A = 0.29$ of Fig.9, 2-periodic orbits (2:1 phase lockings) of the mapping (3) bifurcate from a quasi-periodic orbit. In the presence of noise, the density functions always have two peaks near $A = 0.29$ (c.f. Fig.10); the densities do not change their shape. So, in the presence of noise, we cannot see any stochastic bifurcations of a 2:1 phase

locking. In the next section, we will give an alternative approach which analyzes stochastic bifurcations more quantitatively.

6 Spectral Analysis of Stochastic Bifurcations

The linear operator $\mathcal{P}$ has all the information about the dynamics of the forced oscillator (1). This operator $\mathcal{P}$ (kernel g) is expressed numerically by a matrix. This section analyzes the spectral properties (eigenvalues and eigenfunctions) of this matrix. The operator $\mathcal{P}$ is positive (all elements) and is a stochastic matrix (the sum of every column is unity). Many spectral properties are known about such a positive (or non-negative) matrix (theorem of Perron-Frobenius) and are summarized in (Gantmacher 1959):

(i-a)An irreducible non-negative (stochastic) $n \times n$ matrix A has a real eigenvalue 1 which is a simple root of characteristic equation and the moduli of other eigenvalues do not exceed 1.

(i-b) The 'maximal' eigenvalue 1 has a positive eigenvector and there are no other (linearly independent) non-negative eigenvectors.

(i-c) If A has k eigenvalues λ_0=1, λ_1, ..., λ_{k-1} of modulus unity, these numbers are all distinct roots of $\lambda^k - 1 = 0$ and the whole spectrum λ_0=1, λ_1, ..., λ_{n-1} of A are invariant under a rotation with the angle $2\pi/k$ of the complex plane.

(ii) Moreover, if all elements of A are positive, the maximal eigenvalue 1 exceeds the moduli of all other eigenvalues.

The operator $\mathcal{P}$ with small noise is practically considered to be a non-negative matrix (some elements might be zero practically) although it should be positive theoretically. So it it useful to keep both properties (i) and (ii) in mind.

First we note that the eigenfunction (eigenvector) which belongs to the maximal eigenvalue 1 is the invariant density function h^* of the operator $\mathcal{P}$ and that the eigenvalue with largest modulus other than 1 governs the convergence speed of the sequence $\{h_n\}$ to this invariant density.

Figure 11 shows examples of the whole spectra (eigenvalues) of operators $\mathcal{P}$ with different values of A. In all figures, we can see that the operator has a unique maximum eigenvalue 1. Part (a) corresponds to the deterministic (noise-free) quasi-periodic case (c.f. Fig.9). We can see many complex eigenvalues between zero and unity eigenvalues. Part (b) and (c) correspond to the deterministic 2:1 phase-locking. Comparing (a)-(c), we can see that eigenvalues change their values from complex to real in order of the modulus, which represents a bifurcation from quasi-periodic to 2:1 phase locking in a stochastic sense. Part (d) corresponds to the deterministic 5:3 phase locking (3-periodic orbit of eq. (3)). We can see that the whole spectrum is roughly invariant under an angle $2\pi/3$ rotation of complex plane which is a sign of a stochastic 5:3 phase locking.

In Fig.12, the modulus and the angles of the second eigenvalue of the operator $\mathcal{P}$ are plotted against A values. Note that a bifurcation from quasi-periodic orbits to 2:1 phase lockings occur in the corresponding deterministic case (c.f. Fig.9). Near A=0.35, the second eigenvalue changes its value from complex to real abruptly and the modulus also abruptly changes from decreasing to increasing. Thus we can say that this point is a bifurcation point of a 2:1 phase locking in a stochastic sense. We can convince ourselves of the validity of defining this point as a stochastic bifurcation if we also see the eigenfunction of the second eigenvalue (not shown here). Note that all invariant density functions have the same topological shape (two modes) in this parameter range $0.28 < A < 0.4$. So, we can

observe no stochastic bifurcation in a classical sense (Arnold 1995).

Figure 13 is also a spectral bifurcation diagram corresponding to a deterministic 5:3 phase locking. In this figure, 6th eigenvalues are plotted rather than 2nd ones. In the range of $2.15 \leq A \leq 2.19$, the eigenvalue takes real values. This corresponds to a stochastic bifurcation of 5:3 phase locking. Note that no clear change is observed in the other (from 2nd to 5th) eigenvalues. Not only is the second eigenvalue, but also the other eigenvalues, are important to analyze a stochastic bifurcation.

In Fig.14, angles of the 2nd eigenvalues are plotted in the range of $0.26 < A < 0.44$ with different noise intensities. This corresponds to the spectral bifurcation diagram of Fig.12. The stochastic bifurcation point in the sense of our definition (the point in which the eigenvalue changes its value from complex to real) is shifted rightward as the noise intensity increases.

7 Discussion

We considered the van der Pol relaxation oscillator and its slight modification as a simple model of a neuronal oscillator. We believe this very simple model extracts a certain essential feature of neuronal oscillators. In fact, more physiological (Hodgkin-Huxley-type) model of a Purkinje fiber of a heart has such characteristics as a relaxation oscillator and its waveform resembles to that of the van der Pol oscillator (Noble 1975, Cronin 1987).

We have presented a new method which analyzes the forced relaxation oscillator in the presence of noise. The numerical computation of this method is easy and can be done with any accuracy since this does not use numerical simulation of stochastic differential equations. So, we can analyze very delicate phenomena caused by noise.

Using this method, stochastic bifurcations were analyzed on the basis of spectral properties of a operator. In fact, stochastic bifurcations were clearly observed in the sense of our definition. More intensive discussion on the validity of this definition of a stochastic bifurcation are necessary as future research subjects.

We also briefly discussed the importance of the asymmetry of waveform. A more asymmetrical oscillator seemed to be more easily locked to an input. More intensive investigations about the interplay between the asymmetry and noise is also a future subject of relevance to neurobiology.

References

[1] Special issue on "Stochastic Resonance in Physics and Biology", J. Stat. Phys. 70, Nos. 1/2 (1993)

[2] Arnold, L.: Random Dynamical Systems, In: (Johnson, R. ed.) Dynamical systems, Lecture Notes in Math. vol. 1609, pp.1-43, Springer 1995

[3] Cronin, J.: Mathematical Aspects of Hodgkin-Huxley neural theory, Cambridge University Press 1987

[4] FitzHugh, R.: Impulses and physiological states in theoretical models of nerve membrane, Biophy. J., 1:445-466 (1961)

[5] Gantmacher FR: The Theory of Matrices Vol.II, Chelsea Pub. 1959

[6] Gardiner, C. W.: Handbook of Stochastic Methods for Physics, Chemistry and the Natural Sciences, Springer 1983

[7] Glass, L., Mackey, M. C.: From Clocks to Chaos, The Rhythms of Life, Princeton University Press 1988

[8] Grasman, J.: Asymptotic Methods for Relaxation Oscillations and Applications, Springer 1987

[9] Grasman, J., Jansen, M. J. W.: Mutually synchronized relaxation oscillators as prototypes of oscillating systems in biology, J. Math. Biol. 7, 171-197 (1979)

[10] Grasman, J., Roerdink, J. B. T. M.: Stochastic and chaotic relaxation oscillations, J. Stat. Phys. 54, 949-970 (1989)

[11] Guckenheimer, J., Holmes, P.: Nonlinear Oscillations, Dynamical Systems, and Bifurcation of Vector Fields, Springer 1983

[12] Hodgkin, A.L., Huxley, A.F.: A quantitative description of membrane current and its applications to conduction and excitation in nerve, J. Physiol. 117, 500-544 (1952)

[13] Horsthemke, W., Lefever, R.: Noise-Induced Transitions, Theory and Applications in Physics, Chemistry, and Biology, Springer 1984

[14] Jack, J. J. B., Noble, D., Tsien, R. W.: Electric current flow in excitable cells, Oxford University Press (Clarendon Press) 1975

[15] Kapitaniak, T.: Chaotic Oscillators, World Scientific 1991

[16] Kepler, T. B., Marder, E., Abbott, L. F.: The effect of electrical coupling on the frequency of model neuronal oscillators, Science 248, 83-85 (1990)

[17] Lasota A, Mackey MC: Chaos, Fractals, and Noise: Stochastic Aspects of Dynamics, Springer 1994

[18] Meunier, C.: The electrical coupling of two simple oscillators: load and acceleration effects, Biol. Cybern. 67, 155-164 (1992)

[19] Moss, F., McClintock, P. V. E.: Noise in nonlinear dynamical systems, Vol.1-3, Cambridge Univ. Press 1987

[20] Noble, D.: The Initiation of the Heartbeat, Oxford University Press 1975

[21] Tateno T, Doi S, Sato S, Ricciardi LM: Stochastic phase-lockings in a relaxation oscillator forced by a periodic input with additive noise —A first-passage-time approach— J. Stat. Phys. 78, 917-935 (1995)

[22] van der Pol, B.: On "relaxation-oscillations", Phil. Mag. 2, 978-992 (1926)

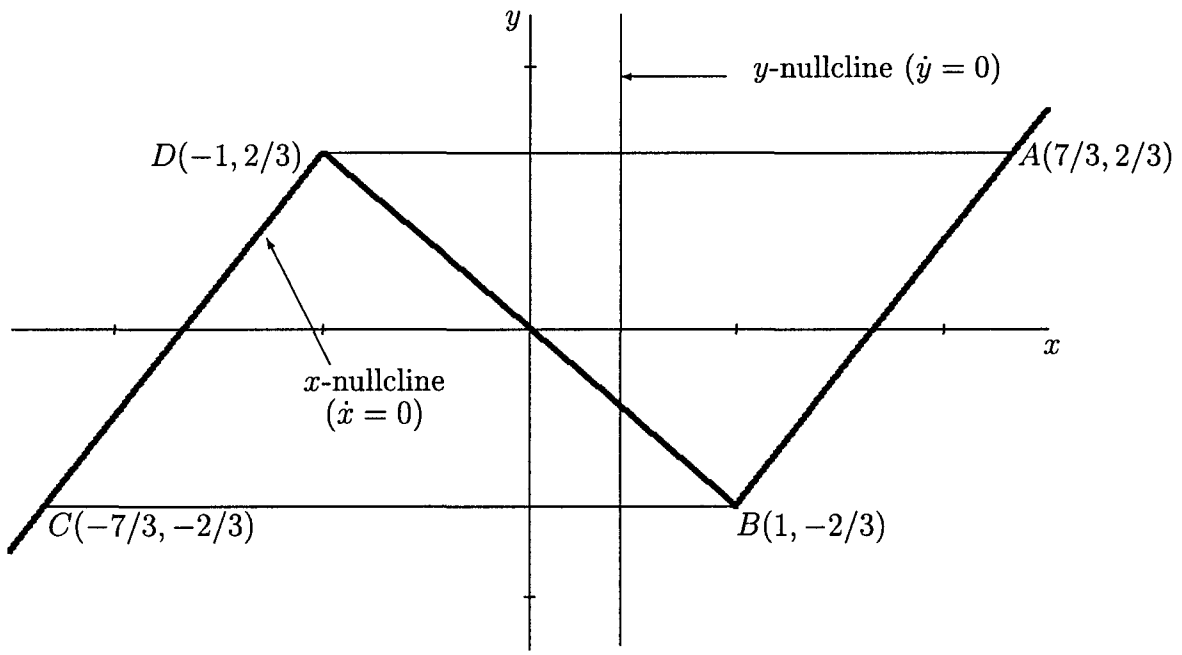

Figure 1: The x-y phase plane of eq. (1) and the N-shaped x-nullcline ($\dot{x}$ =0). The closed orbit ABCD is a limit cycle in the absence of both the periodic input and noise (A=0, $\sigma = 0$). The parameter a shifts the y-nullcline in the horizontal direction ($a = 0.4$ in this figure).

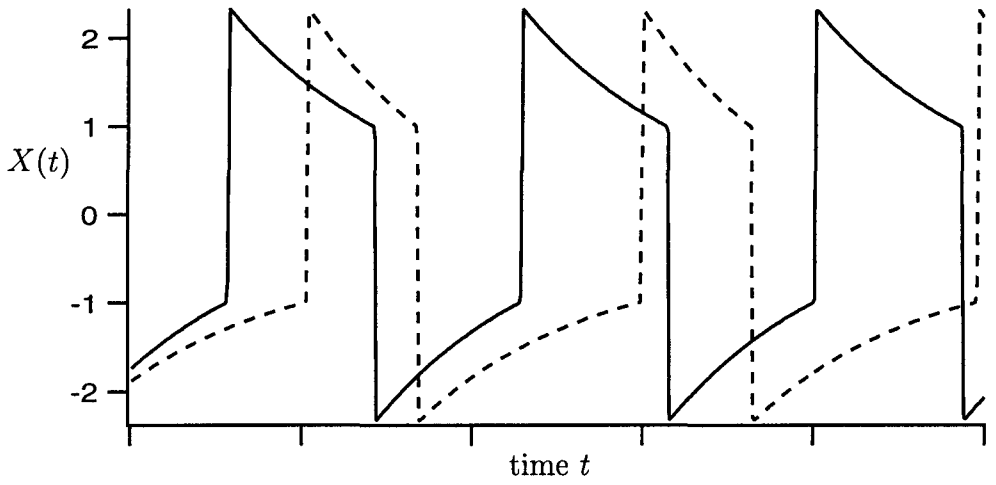

Figure 2: Waveforms of the van der Pol oscillator without both the sinusoidal input and noise for two different parameter values $a = 0$ (solid curve) and $a = -0.5$ (broken curve). As the a value increases, the fraction time such that $X(t) > 0$ decreases and the waveform becomes asymmetric (neuron-like).

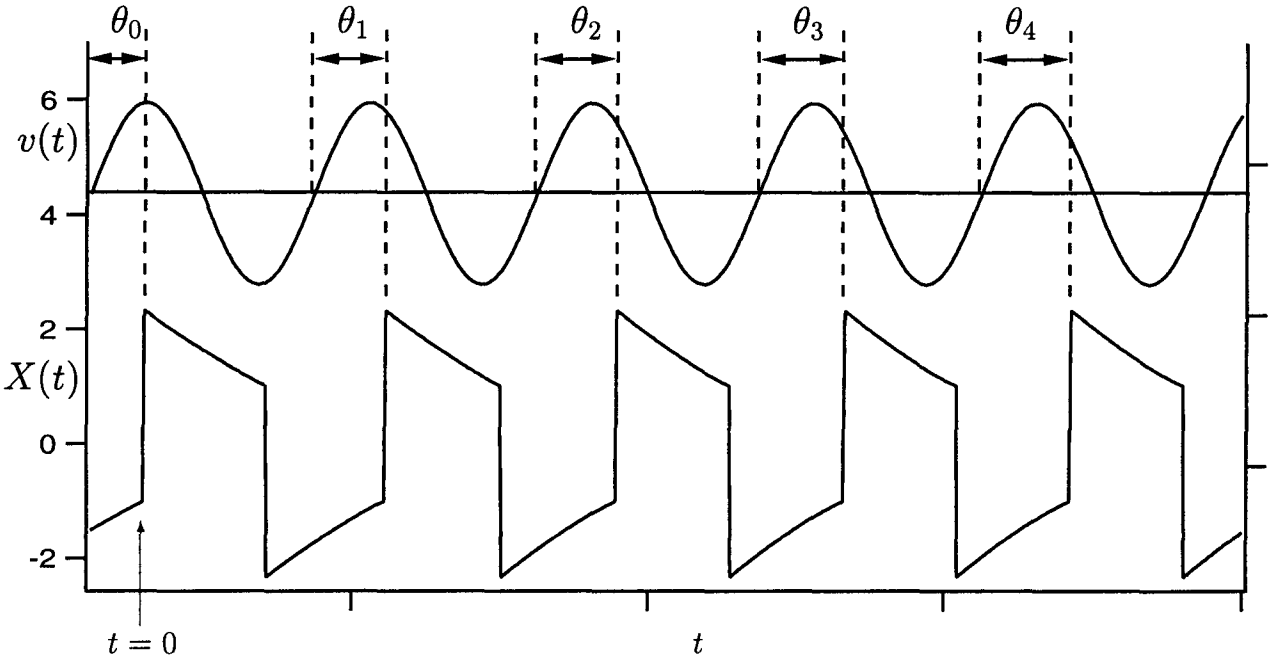

Figure 3: Phase of the sinusoidal input (a 1:1 phase locking). Waveforms of both $X(t)$ and the input $v(t)$ are plotted ($v(t)$ is shifted upward and its scale is arbitrary). $A = 0.3$, $T = 1.5$. The peaks (maximum values) of $X(t)$ corresponds to the point A of the x-y phase plane (Fig.1). At a time $t = 0$, the initial phase of the sinusoidal input is θ_0 and the phase is changed to θ_1, θ_2,... as the time elapses. In this case, the sequence of the phases converges to a certain fixed value θ^*; a 1:1 phase locking occurs.

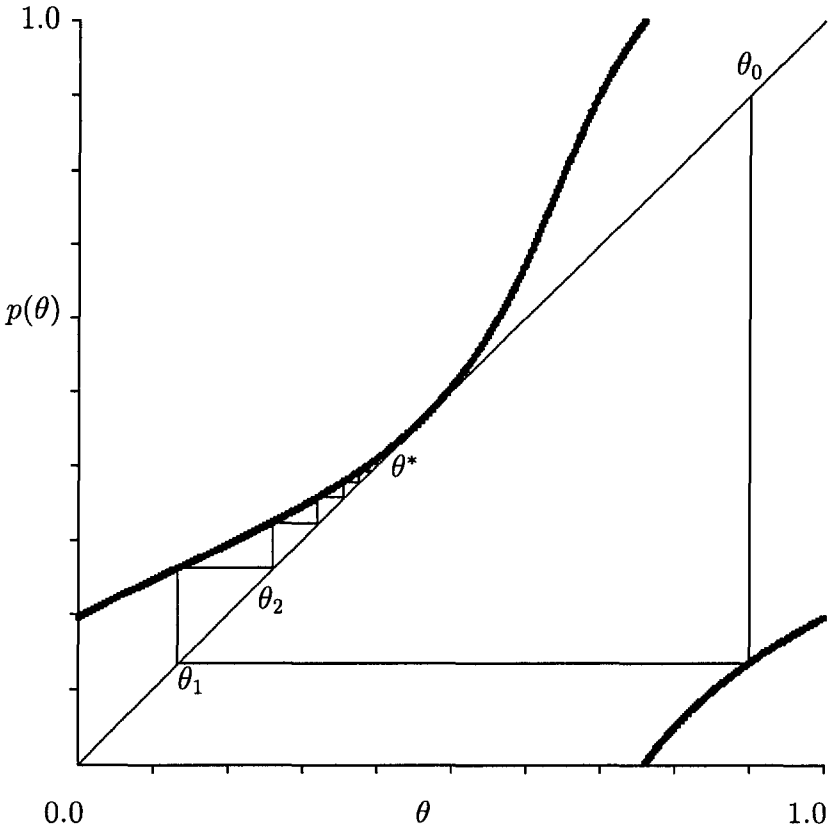

Figure 4: Poincaré map $p(\theta)$ (thick curve) and its orbit $\{\theta_n\}$ (thin lines). A=0.3, T=1.5. The orbit θ_0, θ_1, ... asymptotically converges to a fixed point θ^* which corresponds to a 1:1 phase locking of Fig.3.

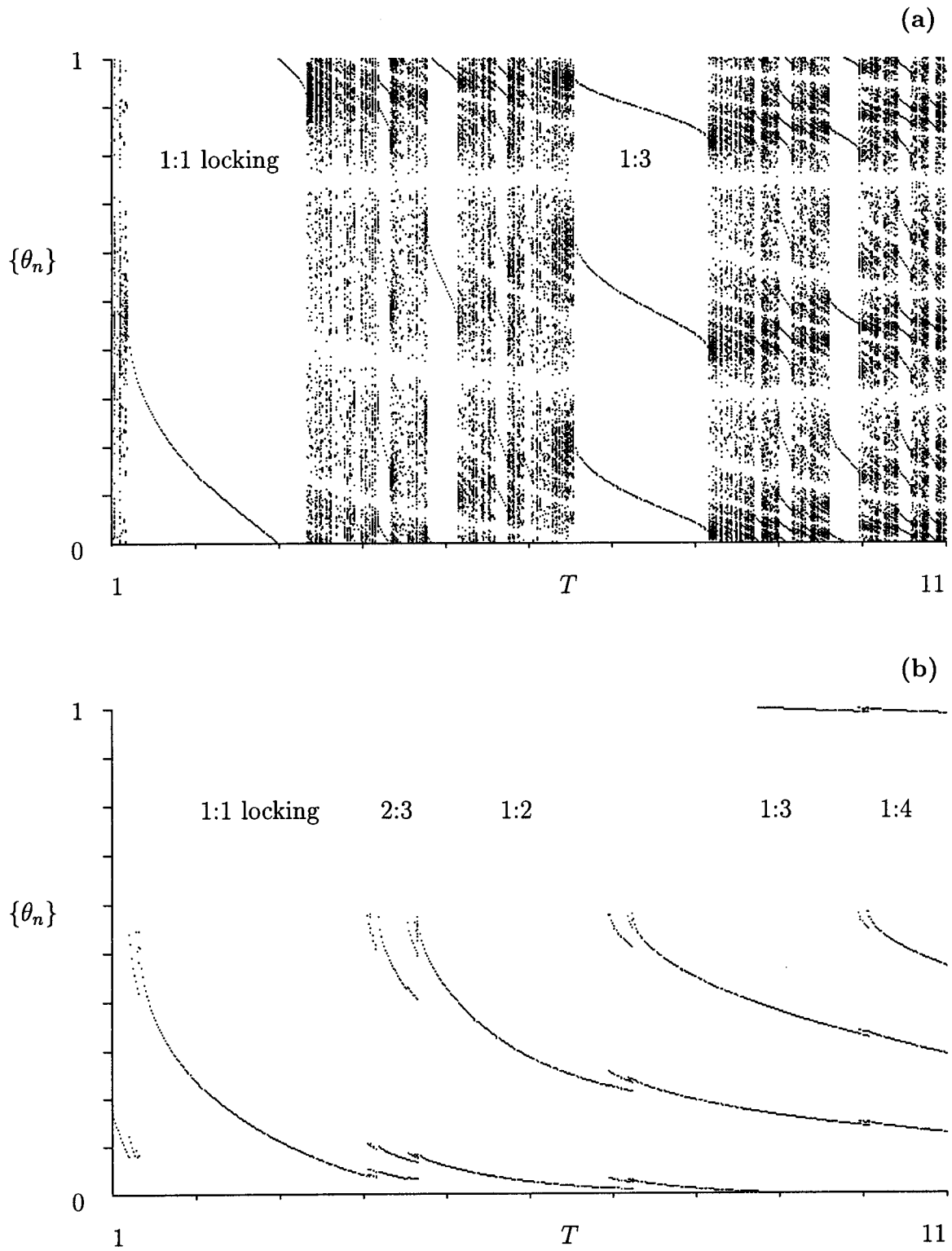

Figure 5: Deterministic bifurcation diagram of the Poincaré map p. $A = 1.0$. A stationary sequence after some transient initial sequence $\{\theta_n\}$, n =101,...,600 produced by eq. (3) were plotted for each of 600 equally spaced T values on the interval $[1, 11]$. **(a)** the original van der Pol ($a = 0$) case. **(b)** Asymmetric ($a = -0.5$) case.

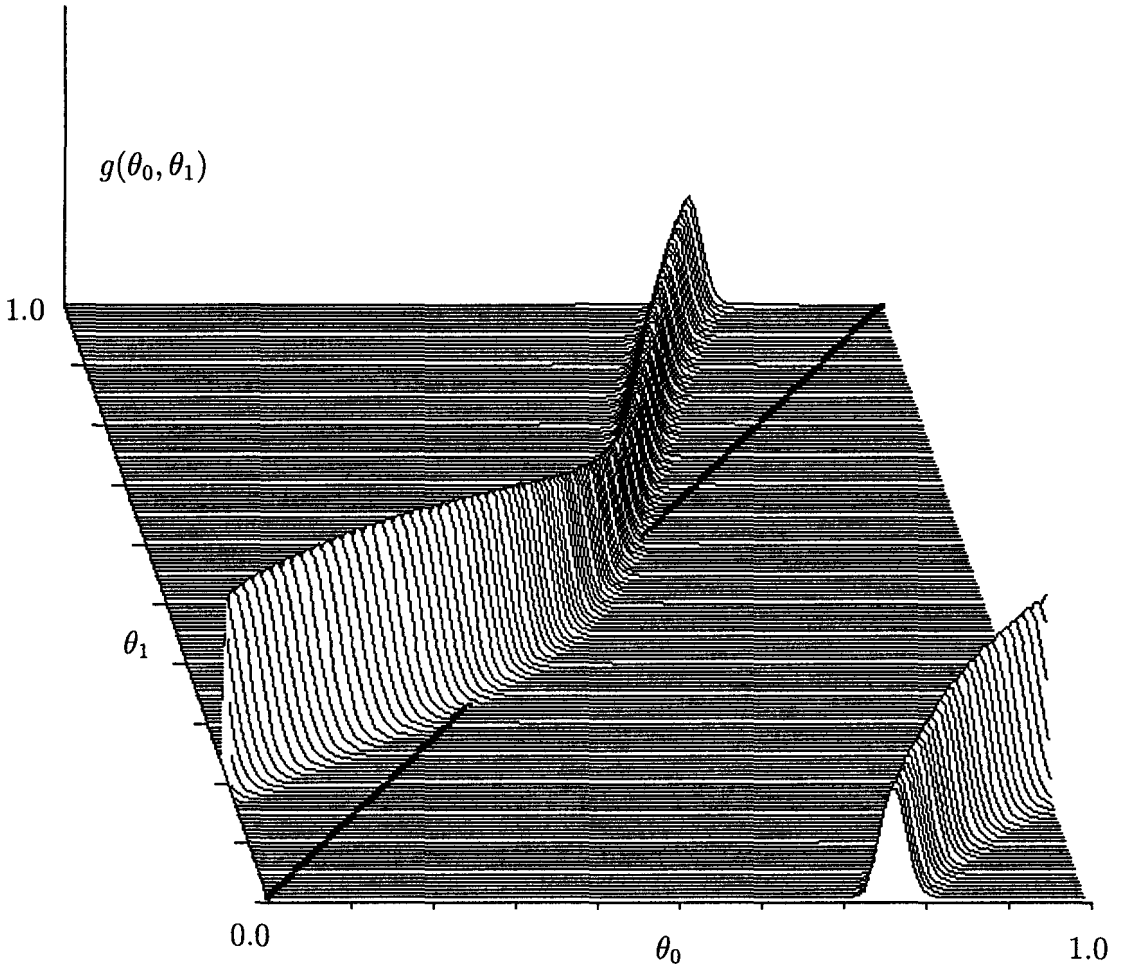

Figure 6: Stochastic kernel function $g(\theta_0, \theta_1)$. $A = 0.3$, $T = 1.5$, $\sigma = 0.03$. This figure corresponds to the deterministic Poincaré map of Fig.4.

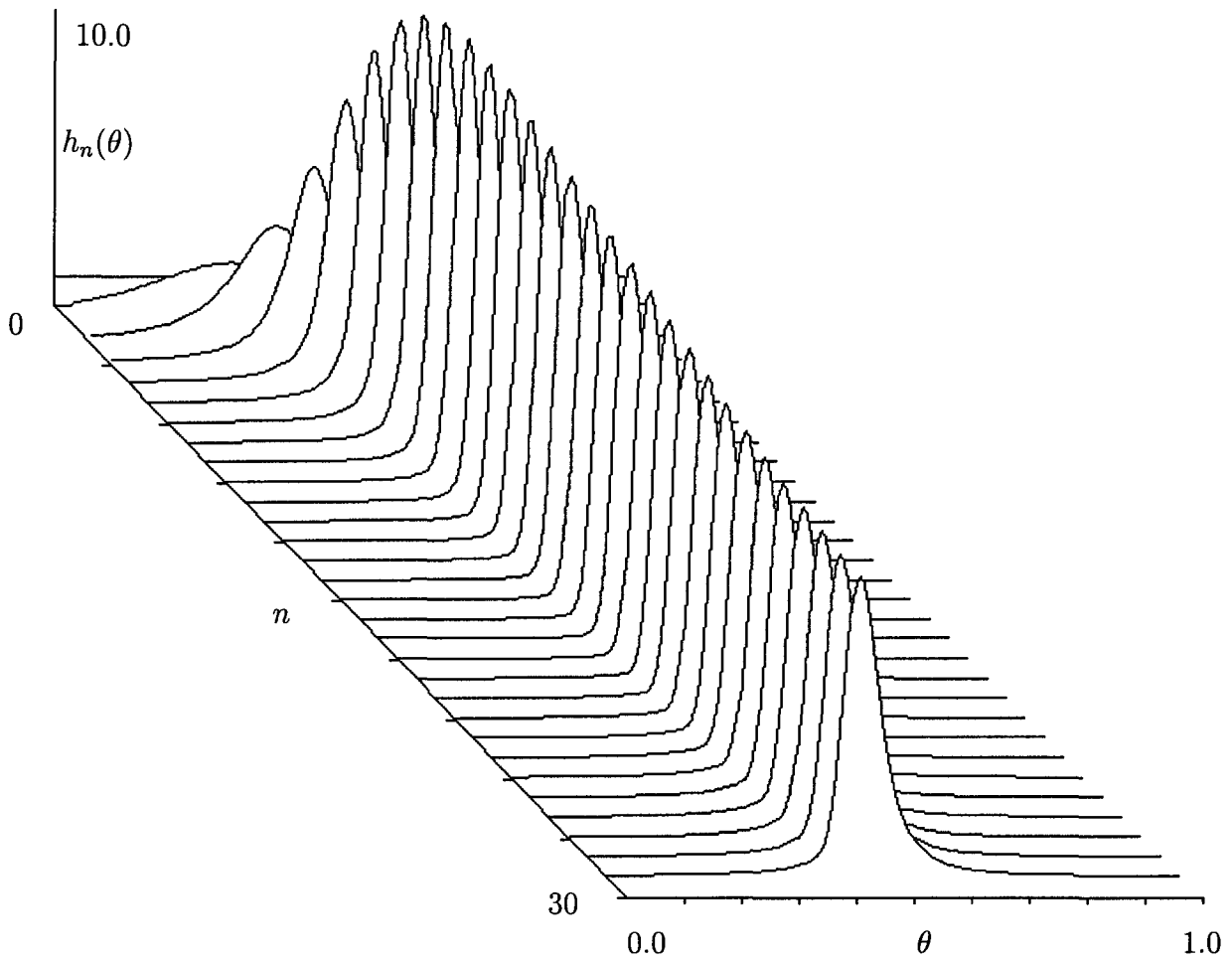

Figure 7: Density evolution (sequence) $\{h_n(\theta)\}$ of a stochastic 1:1 phase-locking. A=0.3, T=1.5, σ=0.03. A uniform initial density function evolves to an invariant density function $h^* \approx h_{30}$.

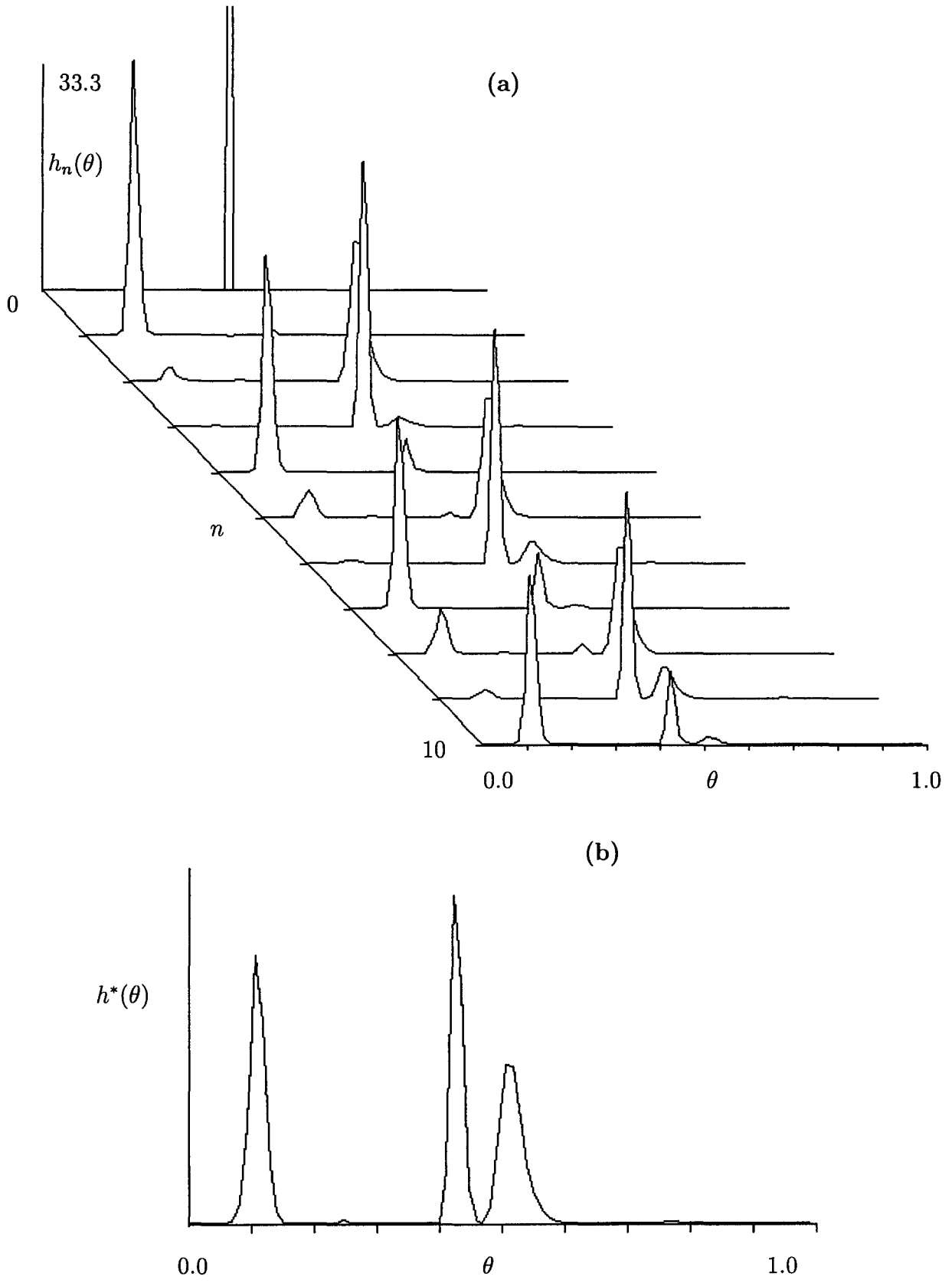

Figure 8: **(a)** Density evolution (sequence) $\{h_n(\theta)\}$ and **(b)** its invariant density $h^* \approx h_{200}$ of a stochastic 5:3 phase locking. A=2.0, T=0.85, σ=0.02.

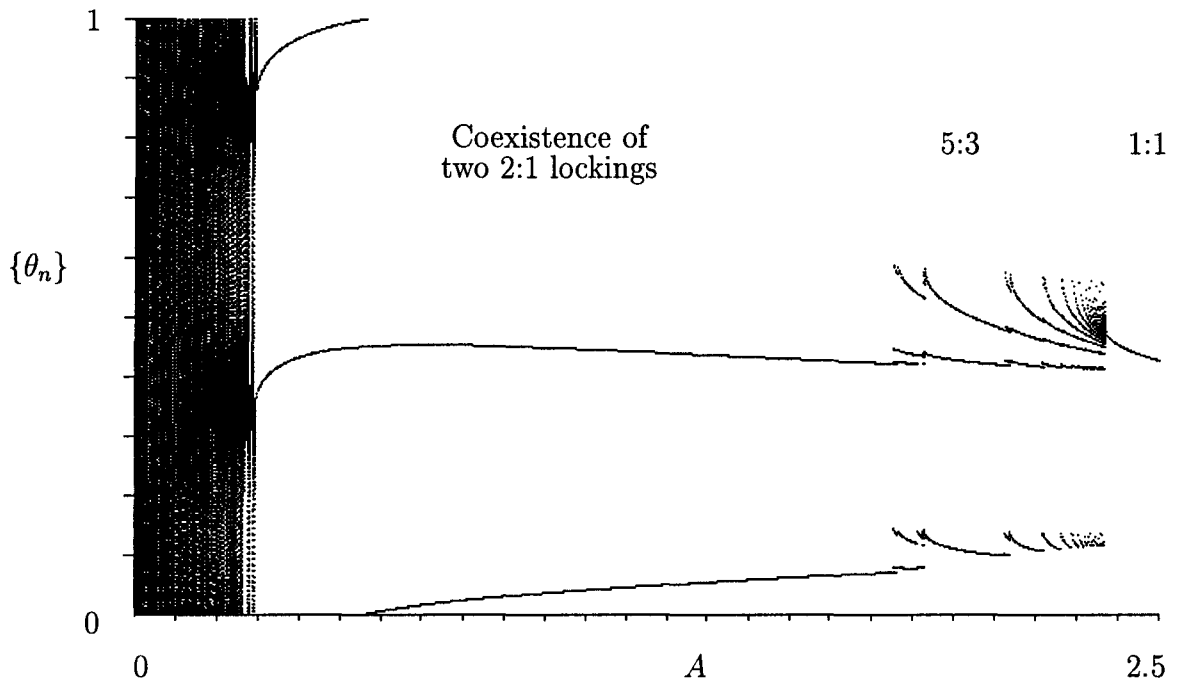

Figure 9: Deterministic bifurcation diagram of the Poincaré map p. $T = 0.85$. A sequence $\{\theta_n\}$, n =101,...,600 produced by eq. (3) were plotted for each of 600 equally spaced A values on the interval $[0, 2.5]$.

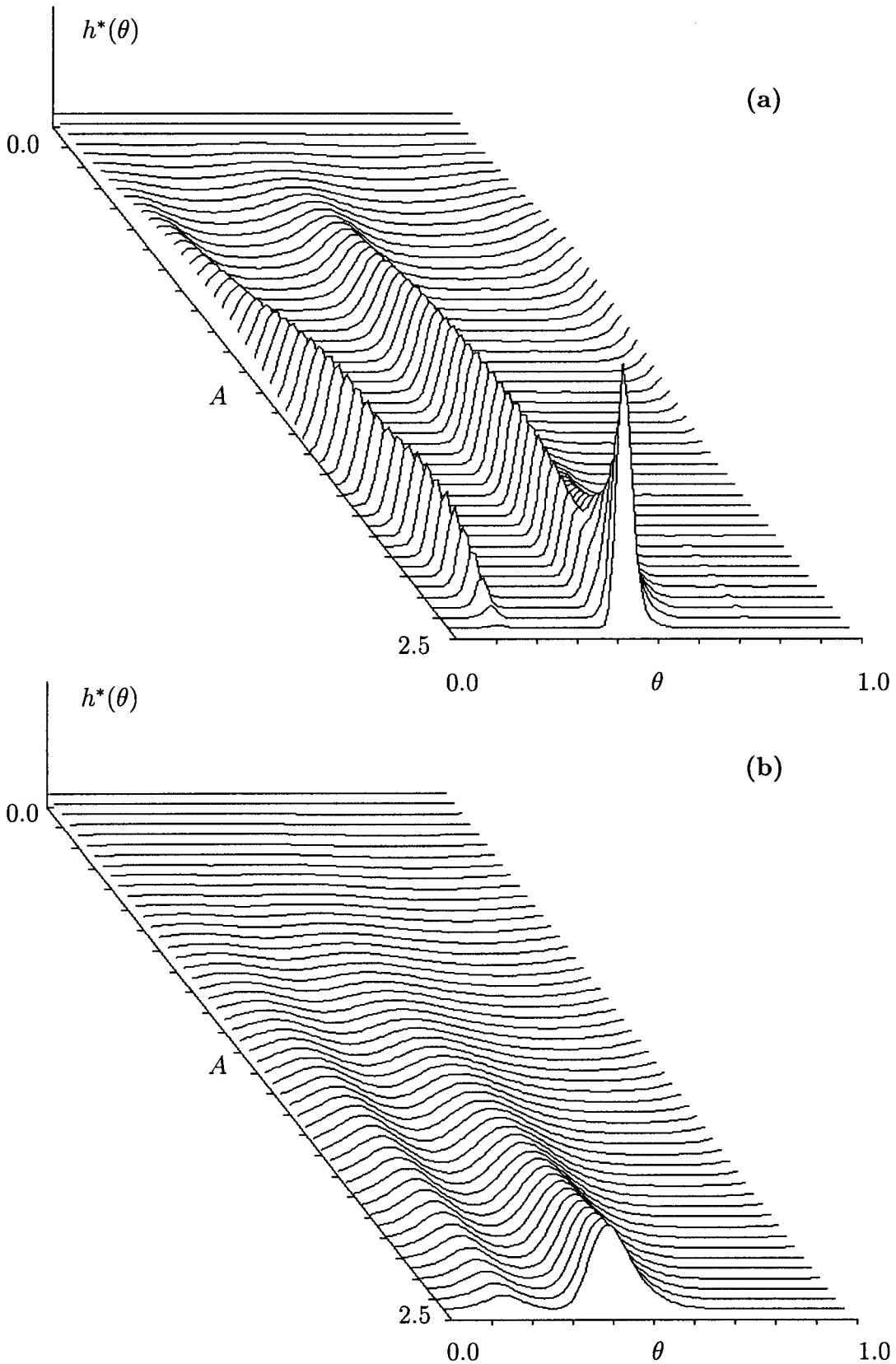

Figure 10: Stochastic (invariant density) bifurcation diagram. $T = 0.85$. Invariant densities $h^*(\theta)$ were plotted for each of 50 equally spaced A values on the interval $[0, 2.5]$. **(a)** σ =0.05

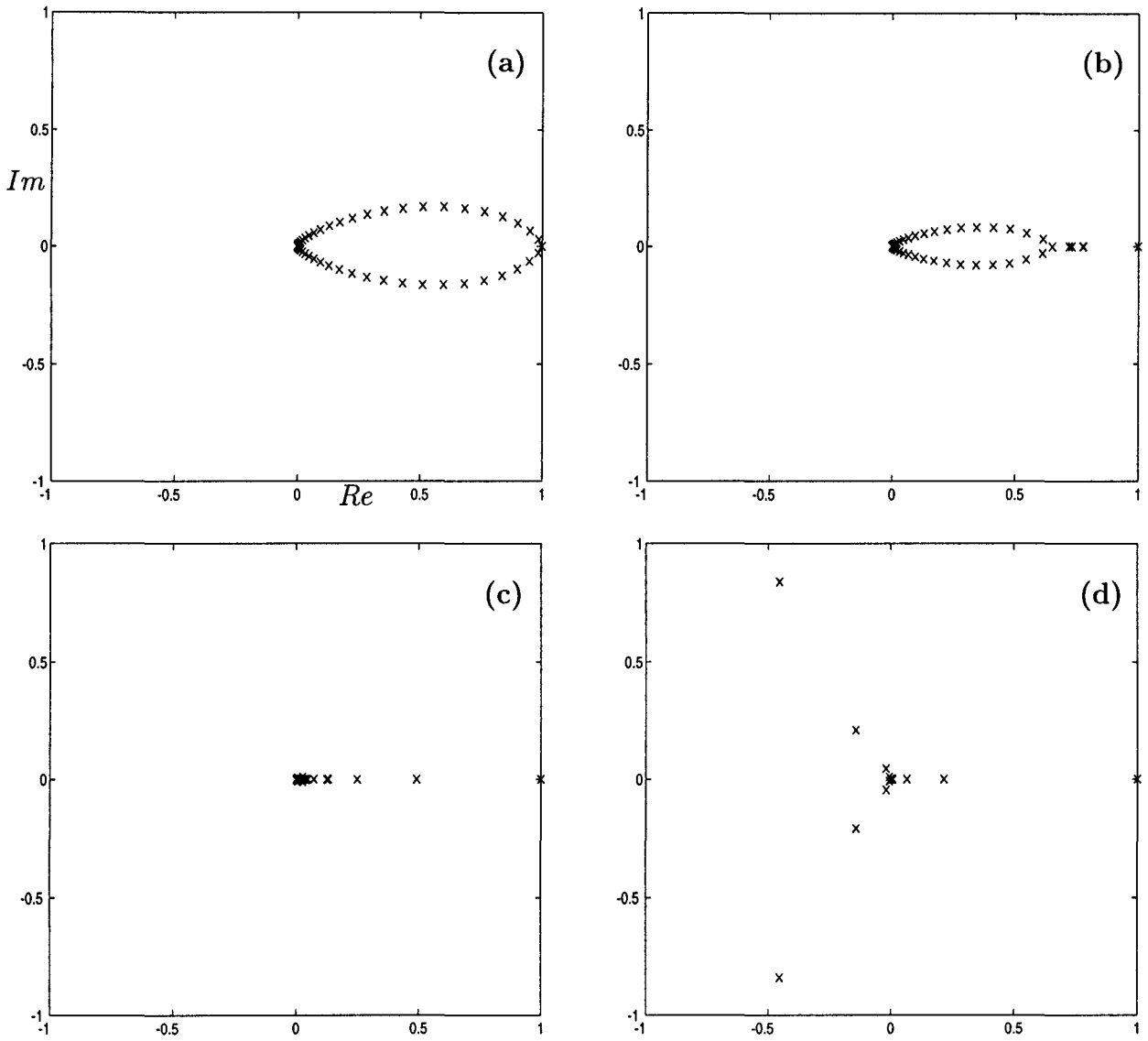

Figure 11: Examples of spectra (eigenvalues) of operators $\mathcal{P}$. T=0.85, σ=0.02 **(a)** A=0.28, quasi-periodic case **(b)** A=0.6, 2:1 locking case **(c)** A=1.0, 2:1 locking case **(d)** A=2.0, 5:3 locking case. The abscissa and the ordinate are the real part and imaginary part of the eigenvalues, respectively.

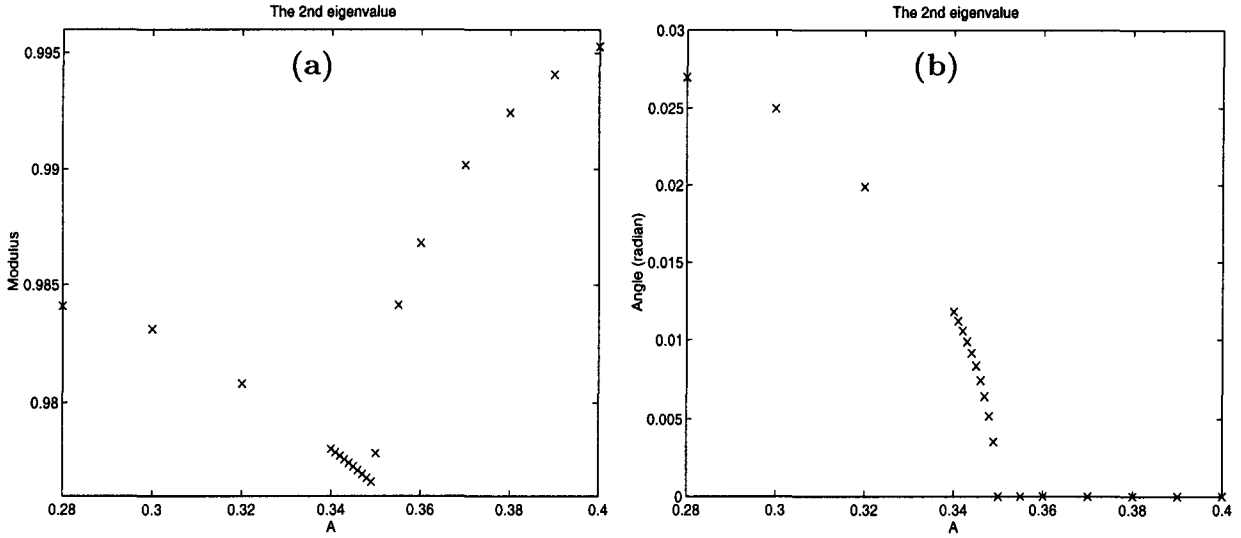

Figure 12: Spectral bifurcation diagram (2:1 locking). **(a)** Modulus and **(b)** angles of the second largest eigenvalues of the operator $\mathcal{P}$ are plotted with various values of the bifurcation parameter $A \in [0.28,0.40]$. T=0.85, σ=0.02. This figure corresponds to the deterministic bifurcation diagram of Fig.9

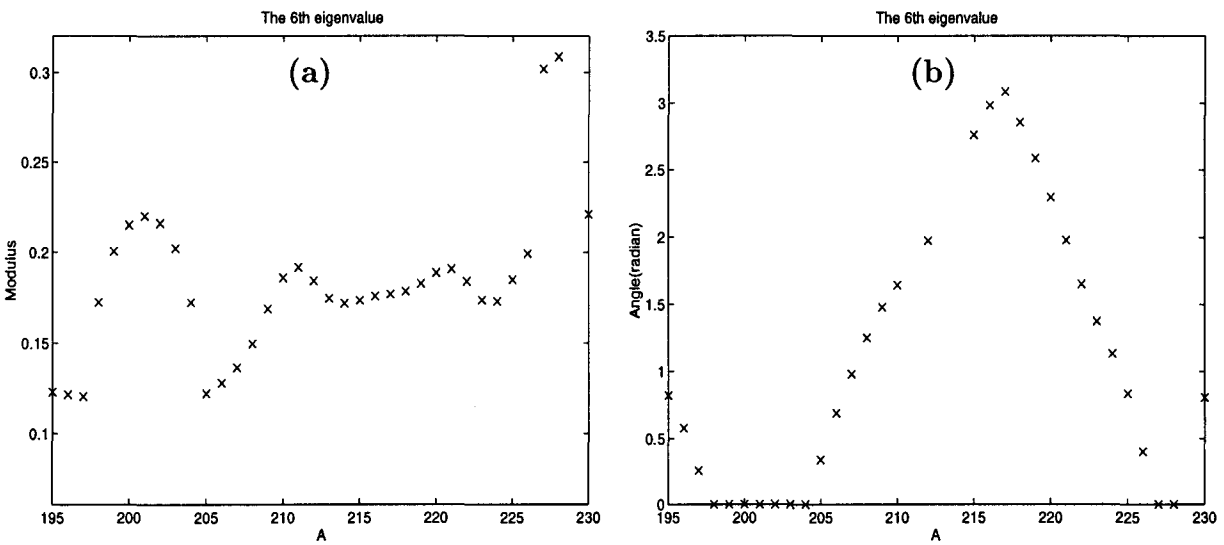

Figure 13: Spectral bifurcation diagram (5:3 locking). **(a)** Modulus and **(b)** angles of the 6th largest eigenvalues of the operator $\mathcal{P}$ are plotted with various values of the bifurcation parameter $A \in [1.95,2.30]$. T=0.85, σ=0.02.

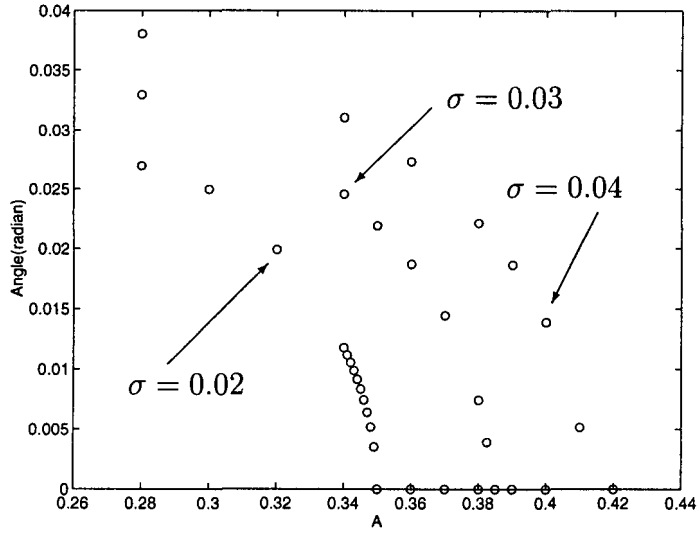

Figure 14: Shift of a stochastic 2:1 bifurcation point. Angles of the 2nd eigenvalues of the operator $\mathcal{P}$ are plotted with different noise intensities σ=0.02, 0.03, 0.04 in the range of $0.26 < A < 0.44$. T=0.85, σ=0.02.